Bounding Solutions of Geometrically Nonlinear Viscoelastic Problems

John M. Stubstad* and George J. Simitses†
Georgia Institute of Technology, Atlanta, Georgia

A method is presented for bounding solutions to problems of linear viscoelastic material behavior formulated using nonlinear kinematic measures of deformation. Upper and lower bounds are established through bounding of the convolution integral of the governing nonlinear Volterra-type integral equation. A significant feature of the manner in which these bounding solutions are generated is that time may be treated as a parameter, thereby casting the bounding solutions into a quasielastic context. Consequently, numerical evaluation is simplified since the necessity of continually approximating convolution integrals of the deformation history, required for exact solution, is eliminated. This, in turn, results in a substantial reduction in the computational effort required for numerical evaluation. In one of the example problems considered, this reduction translates into more than a thirtyfold difference in computer time needed for determination of the exact and bounding solutions. Application of the bounding technique is demonstrated through two examples and includes a limited comparison with some recently published experimental data.

Nomenclature

a	= load eccentricity
E_1, E_2	= elastic constants of ideal viscoelastic material
$g(s,u)$	= Green's function for the spatial integrals
I	= moment of inertia
$J(t)$	= creep compliance
$\mathcal{J}(p)$	= Laplace transform of creep compliance
$k(t-\tau)$	= generic kernel of convolution integral
$K(t)$	= integrated form of $k(t-\tau)$
L	= length of beam
$\mathcal{L}_p$	= Laplace transform operator
$M(s',\tau)$	= bending moment at position s' and time τ
p	= Laplace transform variable
P	= time-independent load
P_E	= Euler load
$R(t)$	= time-dependent load
s', s	= dimensional and nondimensional distance along the beam, respectively
t, τ	= time
x, y	= spatial coordinates
$\alpha(\tau)$	= angle of rotation of the end of the cantilever column
$\Delta(\tau), \delta(\tau)$	= lateral and transverse deflection of the end of the beam, respectively
η_1	= viscous coefficient of ideal viscoelastic material
$\theta(s,t)$	= generic representation of a spatial integral
$\kappa(s',t)$	= curvature at position s' and time t
λ	= scalar parameter
μ	= relaxation constant of ideal viscoelastic material
$\varphi(s',\tau)$	= angle of rotation of the cantilever at position s' and time τ
$\Phi(s',p)$	= Laplace transform of angle of rotation

Subscripts

qe	= quasielastic solution
ub, lb	= upper and lower bounds, respectively

Introduction

INTEGRAL transform techniques, such as the Laplace transform, provide simple and direct methods for solving viscoelastic problems formulated within a context of linear material response and using linear measures for deformation. Application of the transform operator reduces the governing linear integrodifferential equations to a set of algebraic relations between the transforms of the unknown functions, the viscoelastic operators, and the initial and boundary conditions. Inversion, either directly or through the use of the appropriate convolution theorem, provides the time domain response, once the unknown functions have been expressed in terms of sums, products, or ratios of known transforms. When exact inversion is not possible, approximate techniques, such as suggested by Schapery,[1] may provide accurate results.

The overall problem becomes substantially more complex when nonlinear effects must be included. We consider here situations where a linear material constitutive law can still be productively employed, but where the magnitude of the resulting time-dependent deformations warrants the use of a nonlinear kinematic analysis. The governing equations will be nonlinear integrodifferential equations for this class of problems. Thus, traditional as well as approximate techniques, such as cited above, cannot be employed since the transform of a nonlinear function is not explicitly expressible.

Rogers and Lee[2] considered such a problem in an investigation of the finite deflection of a viscoelastic cantilever beam. Employing an analogy of an associated elastic problem, they derived a solution to the viscoelastic problem in a form involving a time convolution of a nonlinear space and time-dependent integral function. Numerical evaluation was accomplished using Picard's method of successive substitutions. Newton-Coates quadratures were employed to approximate the spatially dependent integral relationship; a mean-value-based finite-difference formula was used for the time convolution.

Solution procedures of this type are generally well suited for computer implementation. However, they can become

Received Oct. 26, 1985; presented as Paper 86-0943 at the AIAA/ASME/ASCE/AHS 27th Structures, Structural Dynamics and Materials Conference, San Antonio, TX, May 19-21, 1986; revision received April 7, 1986.

*Graduate Research Assistant, School of Engineering Science and Mechanics.

†Professor, School of Engineering Science and Mechanics. Associate Fellow AIAA.

computationally inefficient when the response must be determined over an extended time period. Each increment in time requires a reevaluation of the convolution integrals. Thus, the entire deformation history must be retained in memory during the calculations. Since each completed set of computations adds another set of results to this history, this generates an ever-increasing memory requirment. In addition, the total number of computations performed during each succeeding iteration also increases.

In this regard, an approximation technique proposed by Schapery[3] can provide an attractive alternative. Commonly referred to as the *quasielastic* approximation, it has most recently been employed by Vinogradov[4] and Vinogradov and Wijeweera[5] in studies of the behavior of eccentrically loaded viscoelastic cantilever columns.

The method is based on the observation that the solution procedure developed by Rogers and Lee[2] may be interpreted as a sequence of short-time interval quasielastic solutions. This suggests that approximate solutions may be generated by replacing the original viscoelastic problem by an "equivalent" time-dependent elastic one. In this replacement problem, the elastic properties are equated to the instantaneous values of the relaxation moduli or creep compliances of the viscoelastic material.

The inherent numerical advantage provided by this technique is that it eliminates the potentially inefficient calculation of convolution integrals. Thus, the speed and efficiency at which the time-dependent response is calculated is independent of elapsed time. The obvious potential disadvantage is that, since it is an approximation, significant differences may exist between the actual response of the viscoelastic body and those predicted quasielastically. In addition, the quasielastic method does not provide a direct method for assessing whether any errors incurred are conservative.

In this paper, we present an approximation technique that provides both upper- and lower-bound predictions for the class of viscoelastic problems under consideration. From these bounds, one may readily deduce when the approximation provides sufficiently accurate results or when more involved techniques must be used. Finally, we demonstrate that solutions for this class of viscoelastic problems can be accomplished within a Laplace transform context, even though the transformed functions cannot be expresssed as explicit functions of the transform variable.

Preliminaries

As a motivation for the development, consider an integral equation of the form

$$\varphi(x,t)=\lambda\int_0^t k(t-\tau)\theta(x,\tau)\,\mathrm{d}\tau \tag{1}$$

where $\varphi(x,\tau)$ and $\theta(x,\tau)$ may be scalar, vector, or tensor functions of position vector x and time τ. We shall assume that the kernel $k(\tau)$ is positive semidefinite over the range of integration and λ is some scalar parameter. In addition, we assume that $k(\tau)$, $\varphi(x,\tau)$, $\theta(x,\tau)$, and their first partial derivatives with respect to τ are continuous over the interval $0^+\leq\tau\leq t$. Finally, we assume that $\varphi(x,\tau)$ and $\theta(x,\tau)$ are continuous with respect to x over some closed domain D and possess continuous first and second partial derivatives with respect to x over at least the interior of the domain.

For the class of problems under consideration, the function $\theta(x,\tau)$ represents a spatial integral in which $\varphi(x,\tau)$ appears in the integrand in a nonlinear manner. Depending upon the boundary conditions, $\theta(x,\tau)$ may also include additive nonlinear forms of $\varphi(x,\tau)$. Thus, Eq. (1) may be viewed as a Volterra-type integral equation of the second kind.

Let us assume that, even before specific solutions have been generated, we are able to infer some information about the general manner in which $\theta(x,\tau)$ behaves. Suppose, for example, that $\theta(x,\tau)$ represents some measure of deflection which (we deduce) must be a nondecreasing function with respect to time. Thus, over the interval $0^+\leq\tau\leq t$, this would imply

$$\theta(x,0^+)\leq\theta(x,\tau)\leq\theta(x,t) \tag{2}$$

This suggests that if we establish the approximate solutions

$$\varphi_{lb}=\lambda\int_0^t k(t-\tau)\theta(x,0^+)\,\mathrm{d}\tau \tag{3a}$$

$$\varphi_{ub}=\lambda\int_0^t k(t-\tau)\theta(x,t)\,\mathrm{d}\tau \tag{3b}$$

where subscripts *ub* and *lb* denote upper and lower bounds, respectively, we can then define difference functions $\Delta\varphi_{lb}$ and $\Delta\varphi_{ub}$ by

$$\Delta\varphi_{lb}=\varphi(x,t)-\varphi_{lb} \tag{4a}$$

$$\Delta\varphi_{ub}=\varphi_{ub}-\varphi(x,t) \tag{4b}$$

Then substitution of Eqs. (1) and (3) into Eq. (4) yields

$$\Delta\varphi_{lb}=\lambda\int_0^t k(t-\tau)\,[\theta(x,\tau)-\theta(x,0^+)]\,\mathrm{d}\tau \tag{5a}$$

$$\Delta\varphi_{ub}=\lambda\int_0^t k(t-\tau)\,[\theta(x,t)-\theta(x,\tau)]\,\mathrm{d}\tau \tag{5b}$$

As a direct consequence of Eq. (2), the quantities enclosed by square brackets in Eqs. (5) must be positive semidefinite for all values of time τ. Because both $\theta(x,0^+)$ and $\theta(x,t)$ are constant with respect to τ, the square bracket terms must be continuous in τ since, by prior assumption, $\theta(x,\tau)$ is continuous in τ. Thus, for a continuous and positive semdefinite kernel, the integrand is continuous and positive semidefinite over the entire range of integration. Consequently, for positive λ, the differences $\Delta\varphi_{lb}$ and $\Delta\varphi_{ub}$ must be positive for all time. Therefore, the approximate solution φ_{ub} must represent an upper bound for the exact solution. Similarly, φ_{lb} must inherently bound the exact solution from below.

The numerical advantages provided by working with the bounding functions are easily demonstrated. Letting

$$K(t)=\lambda\int_0^t k(t-\tau)\,\mathrm{d}\tau \tag{6}$$

and noting that $\theta(x,0^+)$ and $\theta(x,t)$ are independent of τ imply that Eqs. (3) have the form

$$\varphi_{lb}=K(t)\theta(x,0^+) \tag{7a}$$

and

$$\varphi_{ub}=K(t)\theta(x,t) \tag{7b}$$

Thus, the time convolution of the exact solution [Eq. (1)] has, in the bounding formulation, been replaced by a format in which time appears only as a parameter. Consequently, numerical solution of Eqs. (7) requires integration only over the spatial coordinates, whereas the exact solution requires both spatial and temporal integrations.

The preceding development was based upon the assumption that $\theta(x,\tau)$ was a nondecreasing function with respect to time. The technique is easily adapted to cases where $\theta(x,\tau)$ is a nonincreasing function. Thus, if

$$\theta(x,0^+)\geq\theta(x,\tau)\geq\theta(x,t) \tag{8}$$

we can replace Eqs. (3) with

$$\varphi_{lb} = \lambda \int_0^t k(t-\tau)\theta(x,t)\,d\tau \tag{9a}$$

and

$$\varphi_{ub} = \lambda \int_0^t k(t-\tau)\theta(x,0^+)\,d\tau \tag{9b}$$

Thereafter, proceeding as before generates the desired bounding behavior. In a similar manner, a simple series of modifications to the definitions of the bounding functions are needed when λ is a negative rather than positive scalar.

Applications of the bounding technique, including comparisons with exact solutions, are provided in the following sections.

Applications

End-Loaded Cantilever Beam

As noted earlier, Rogers and Lee[2] developed the first, and a numerically exact, solution for the problem of an end-loaded linearly viscoelastic cantilever beam. The solution, in the general form of Eq. (1), was evaluated by employing Newton-Coates quadratures for the spatially dependent integral function $\theta(x,\tau)$ and a mean value based finite-difference formula for the convolution with $k(t-\tau)$. Several years later, Schapery,[3] in a paper describing the quasielastic method, presented an approximate solution for this problem. Since this approximate solution was in the form of Eqs. (7), Schapery was able to generate numerical results directly from the elastic analysis presented in Ref. 2. Thus, his solution required only numerical evaluation of a spatially dependent integral equation with time treated as a parameter.

Here, we analyze the same problem using the bounding procedure. It is demonstrated that Schapery's approximate solution is, in fact, a lower-bound solution for a suitably restricted range of deformation. In addition, it is shown that a reasonably close upper-bound solution may be readily obtained.

Derivation of the governing integrodifferential equation is documented in Ref. 2 and thus only summarized here. The beam is assumed to be thin and composed of a linearly viscoelastic material. Its geometry in the deformed configuration is illustrated in Fig. 1. The loading is assumed to be applied quasistatically and thus inertia terms are neglected.

Reference line extensional strains are assumed to be negligibly small. Thus, a coordinate s' is employed to specify position in both the initial and the deformed states. A nondimensional coordinate s is defined by dividing s' by the beam length L. Assuming a linear distribution of strains through the depth, bending thus occuring within a Bernoulli-Euler context, results in the moment-curvature relationship given by

$$\kappa(s',t) = \left(\frac{1}{I}\right)\int_{-\infty}^{t} J(t-\tau)\left[\frac{\partial M(s',\tau)}{\partial \tau}\right]d\tau \tag{10}$$

where $\kappa(s',t)$ denotes the curvature and $M(s',\tau)$ the bending moment at location s'. I is the moment of inertia of the beam and $J(t)$ the creep compliance of the material. The moment at position s' is given by

$$M(s',\tau) = R(\tau)\,[L - x(s',\tau) - \Delta(\tau)] \tag{11}$$

where $R(\tau)$ is the end load (see Fig. 1).

From kinematic considerations, we note that

$$\kappa(s',t) = \frac{\partial \varphi(s',t)}{\partial s'} \tag{12a}$$

$$\frac{\partial x(s',t)}{\partial s'} = \cos\varphi(s',t) \tag{12b}$$

$$\frac{\partial y(s',t)}{\partial s'} = \sin\varphi(s',t) \tag{12c}$$

Substitution of Eqs. (11) and (12a) into Eq. (10), differentiation with respect to s' and use of Eq. (12b) yield, after nondimensionalization

$$\frac{\partial^2 \varphi(s,t)}{\partial s^2} = -\left(\frac{L^2}{I}\right)\int_{-\infty}^{t} J(t-\tau)\left\{\frac{\partial [R(\tau)\cos\varphi(s,\tau)]}{\partial \tau}\right\}d\tau \tag{13}$$

The associated boundary conditions are

$$\varphi(0,t) = 0 \tag{14a}$$

$$\frac{\partial \varphi(1,t)}{\partial s} = 0 \tag{14b}$$

It is assumed the beam is undeformed for $\tau < 0$. Then, by taking the Laplace transform of Eqs. (13) and (14), we obtain

$$\frac{\partial^2 \Phi(s,p)}{\partial s^2} = -\left(\frac{L^2}{I}\right) p\mathcal{J}(p)\,\mathcal{L}_p[R(\tau)\cos\varphi(s,\tau)] \tag{15a}$$

$$\Phi(0,p) = 0 \tag{15b}$$

$$\frac{\partial \Phi(1,p)}{\partial s} = 0 \tag{15c}$$

where $\mathcal{L}_p[\ ]$ is the Laplace transform operator, p the transform variable, and $\mathcal{J}(p)$ and $\Phi(s,p)$ the transforms of $J(t)$ and $\varphi(s,t)$, respectively. Here, we have tacitly assumed that the Laplace transform of the expression within the brackets exists, in the usual sense, even though a formal expression for it is not available.

Assuming that the transform variable appears only as a parameter, Eq. (15a) can be viewed as a type of *ordinary* differential equation. Integration thus yields

$$\frac{\partial \Phi(s,p)}{\partial s} - \frac{\partial \Phi(0,p)}{\partial s} = -\left(\frac{L^2}{I}\right) p\mathcal{J}(p)\int_0^s \left[\int_0^\infty e^{-p\tau} R(\tau)\cos\varphi(u,\tau)\,d\tau\right]du \tag{16}$$

where the Laplace transform has been expressed in the explicit manner. Application of the boundary condition, as

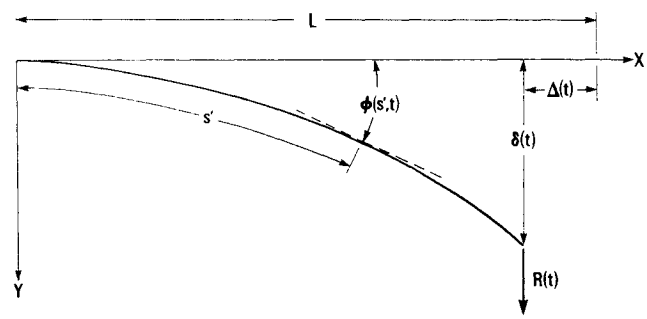

Fig. 1 Geometry of the end-loaded cantilever beam.

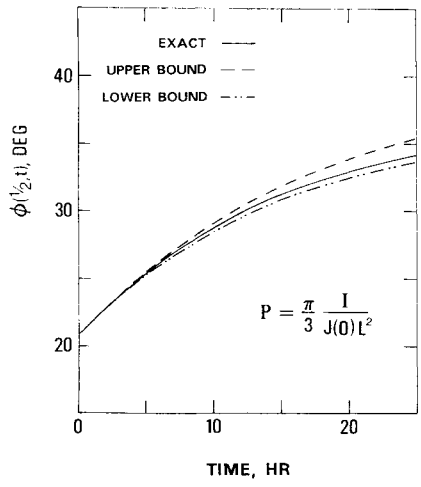

a) At midspan.

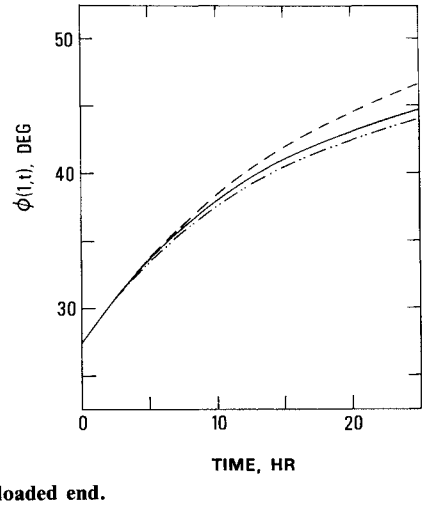

b) At loaded end.

Fig. 2 Angle of deflection of the end-loaded cantilever beam.

given by Eq. (15c), yields

$$\frac{\partial\Phi(0,p)}{\partial s}=\left(\frac{L^2}{I}\right)p\mathcal{J}(p)\int_0^\infty e^{-p\tau}R(\tau)\left[\int_0^1\cos\varphi(u,\tau)\mathrm{d}u\right]\mathrm{d}\tau \tag{17}$$

Note that we have interchanged the order of integration of Eq. (16). This follows directly from the assumption of inextensionality; therefore, s and τ represent independent variables. Substitution of Eq. (17) into Eq. (16) yields

$$\frac{\partial\Phi(s,p)}{\partial s}=-\left(\frac{L^2}{I}\right)p\mathcal{J}(p)\int_0^\infty e^{-p\tau}R(\tau)\times\left[\int_1^s\cos\varphi(u,\tau)\mathrm{d}u\right]\mathrm{d}\tau \tag{18}$$

Integration of Eq. (18) with respect to s, use of the boundary condition [Eq. (15b)], and manipulation as before yield

$$\Phi(s,p)=-\left(\frac{L^2}{I}\right)p\mathcal{J}(p)\int_0^\infty e^{-p\tau}R(\tau)\times\left[\int_0^s\int_1^r\cos\varphi(u,\tau)\mathrm{d}u\mathrm{d}r\right]\mathrm{d}\tau \tag{19}$$

The term in the brackets may be simplified through integration by parts and by employing

$$g(s,u)=u,\quad 0\le u\le s$$
$$=s,\quad s\le u\le 1 \tag{20}$$

to yield

$$\Phi(s,p)=\left(\frac{L^2}{I}\right)p\mathcal{J}(p)\mathcal{L}_p\left[R(\tau)\int_0^1 g(s,u)\cos\varphi(u,\tau)\mathrm{d}u\right] \tag{21}$$

Thus defining $\theta(s,\tau)$ by

$$\theta(s,\tau)=\int_0^1 g(s,u)\cos\varphi(u,\tau)\mathrm{d}u \tag{22}$$

results in

$$\Phi(s,p)=(L^2/I)p\mathcal{J}(p)\mathcal{L}_p[R(\tau)\theta(s,\tau)] \tag{23}$$

Next, the Laplace convolution theorem is employed to invert Eq. (23) to yield

$$\varphi(s,t)=\left(\frac{L^2}{I}\right)\int_0^t J(t-\tau)\frac{\partial[R(\tau)\theta(s,\tau)]}{\partial\tau}\,\mathrm{d}\tau \tag{24}$$

Upon a final integration by parts we have

$$\varphi(s,t)=\left(\frac{L^2}{I}\right)\left[J(0)R(t)\theta(s,t)+\int_0^t J'(t-\tau)R(\tau)\theta(s,\tau)\mathrm{d}\tau\right] \tag{25}$$

where $(\,)'$ denotes differentiation with respect to the argument of the function. Note that Eq. (25) is the viscoelastic solution reported in Ref. 2.

Bounding solutions are developed in the following manner. Provided, after quasistatic application, the load $R(\tau)$ is held constant at some value P, it is reasonable to presume that the angle of deflection $\varphi(s,\tau)$ will be a nondecreasing function in time. Thus, for the interval $0^+\le\tau\le t$,

$$\varphi(s,0^+)\le\varphi(s,\tau)\le\varphi(s,t) \tag{26}$$

Consequently, restricting our attention to a range of deflection such that $0\le\varphi\le\pi/2$ we may conclude that

$$\cos\varphi(s,0^+)\ge\cos\varphi(s,\tau)\ge\cos\varphi(s,t) \tag{27}$$

Thus, from Eqs. (22) and (27) we have

$$\theta(s,0^+)\ge\theta(s,\tau)\ge\theta(s,t) \tag{28}$$

Through the use of Eq. (28), we can bound the convolution integral of Eq. (25) as follows:

$$P\theta(s,0^+)\int_0^t J'(t-\tau)\mathrm{d}\tau\ge\int_0^t J'(t-\tau)R(\tau)\theta(s,\tau)\mathrm{d}\tau\ge P\theta(s,t)\int_0^t J'(t-\tau)\mathrm{d}\tau \tag{29}$$

Integration of the first and third integrals in Eq. (29) and substitution of these results into Eq. (25) yield, after rearrangement,

$$\varphi_{lb}(s,t)=J(t)\left(\frac{PL^2}{I}\right)\theta(s,t) \tag{30a}$$

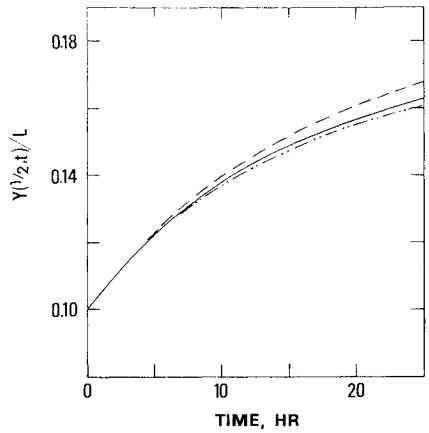

a) At midspan.

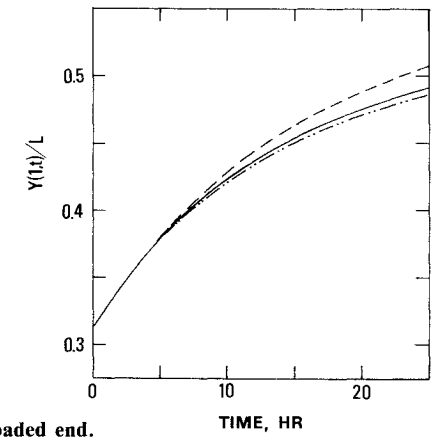

b) At loaded end.

Fig. 3 Vertical deflection of the end-loaded cantilever beam.

$$\varphi_{ub}(s,t) = J(0)\left(\frac{PL^2}{I}\right)\left\{\theta(s,t) + \left[\frac{J(t)}{J(0)} - 1\right]\theta(s,0^+)\right\} \tag{30b}$$

Note that Eq. (30a) is the quasielastic solution proposed by Schapery.

Bounding of the deflection of the beam can be readily accomplished by using Eqs (30). Nondimensionalization and then integration of Eq. (12c) yield

$$\frac{y(s,t)}{L} = \int_0^s \sin\varphi(u,t)\,du \tag{31}$$

Thus, since $\varphi_{lb}(s,t) \le \varphi(s,t) \le \varphi_{ub}(s,t)$, we note that, for $0 \le \varphi \le \pi/2$

$$\sin\varphi_{lb}(s,t) \le \sin\varphi(s,t) \le \sin\varphi_{ub}(s,t) \tag{32}$$

which yield, upon substitution into Eq. (31)

$$\frac{y_{lb}(s,t)}{L} = \int_0^s \sin\varphi_{lb}(u,t)\,du \tag{33a}$$

$$\frac{y_{ub}(s,t)}{L} = \int_0^s \sin\varphi_{ub}(u,t)\,du \tag{33b}$$

Numerical solutions of Eqs. (25), (30), and (33) are generated in a manner similar to Ref. 2. Picard's method of successive substitutions is employed to numerically solve the integral equations, Eqs. (25) and (30). Spatial integrals are approximated by using Newton-Coates formulas; a fixed-step trapezoidal rule is used for the time convolution. All computations are performed on a CDC Cyber 180/855 located at the Georgia Institute of Technology.

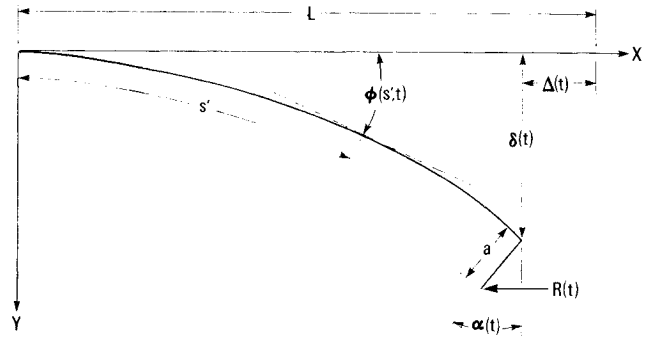

Fig. 4 Geometry of the eccentrically loaded cantilever column.

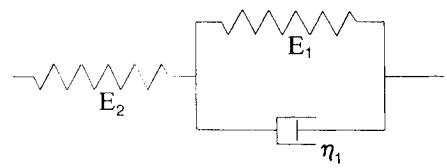

Fig. 5 Ideal three-element "limited" creep model.

Figures 2 and 3 compare the results obtained with the bounding formulation to the exact solution for the loading case reported in Refs. 2 and 3. The form of the creep compliance for this example is

$$J(t)/J(0) = 1 + 7.6\times10^{-4}t + 1.12(1 - e^{-0.055t}) \tag{34}$$

Figure 2 demonstrates that the bounding solutions provide a reasonably narrow band at both the midspan and the loaded end locations. For this particular case, the lower bound tends to more closely approximate the actual solution. For both the upper and lower bounds, the discrepancy between the approximate result and the exact solution tends to increase with elapsed time and distance from the clamped end.

Figure 3 compares the calculated vertical deflections at midspan and at the loaded end. It can be noted that the descrepancies between the bounding and exact solutions behave in the same manner as described above. In terms of absolute accuracy, after 24 h, the upper-bound end deflection exceeds the exact result by approximately 3.3%. The lower bound, at the same point and time, is only 1.2% less than the exact deflection. Using a 0.1 h fixed-length time step, the exact solution required 15.6s of CPU time to compute. Calculated for the same number of time intervals, each of the bounding solutions required only 4.1 CPU s. Note, however, that the accuracy of the bounding solutions is independent of the length of the time step. Thus, identical bounding solution results can be obtained with, for example, a 1.0 h time step. Using this larger time step, the computation time for each of the bounding solutions was reduced to only 0.5 CPU s. Accurate results could not be obtained from the exact solution using a time step this large due to errors in approximating the convolution integrals.

Eccentrically Loaded Cantilever Column

Although formally similar to the prior example, this problem is of interest because the eccentric loading generates additive nonlinear boundary terms in the general solution. The presence of these terms substantially influences the accuracy of the predictions of the system response.

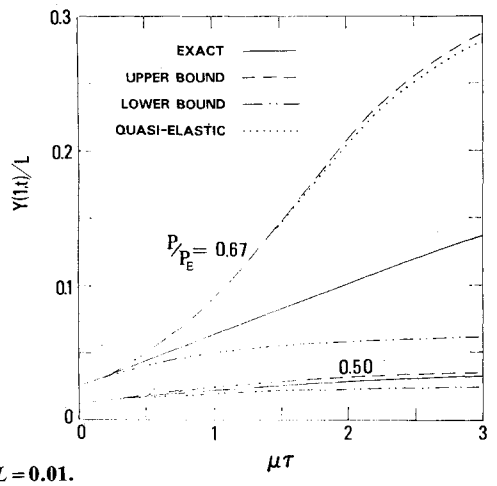

a) $a/L=0.01$.

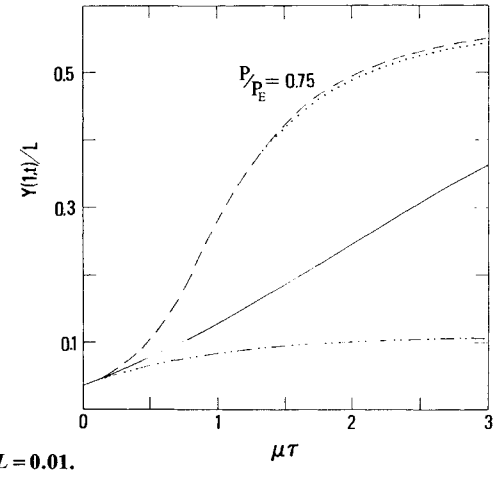

b) $a/L=0.01$.

Fig. 6 End deflection of the eccentrically loaded cantilever column for the three-element model.

A quasielastic solution of this problem was recently presented by Vinogradov.[4] Included with the analysis were numerical results for two ideal constitutive models, using two eccentricity ratios and a wide range of applied loads. Subsequently, Vinogradov and Wijeweera[5] and Wijeweera[6] published comparisons of results obtained using the quasielastic approximation of Ref. 4 to experimental data from tests conducted on PTFE G-700 columns. The loading and eccentricity ratios employed in those tests were, however, restricted to relatively narrow ranges in value.

Bounding solutions for the problem are developed in a similar manner to the prior example. The column is assumed to be inextensional, linearly viscoelastic, and loaded quasistatically. Its geometry in the deformed configuration is illustrated in Fig. 4. Note that the applied load remains parallel to the x axis.

For this geometry, the moment at any position s' is given by

$$M(s',\tau)=R(\tau)\,[\delta(\tau)+a\cos\alpha(\tau)-y(s',\tau)] \tag{35}$$

Substitution of Eq. (35) into Eq. (10), differentiation with respect to s', use of Eqs. (12a) and (12c) followed by nondimensionalization yield

$$\frac{\partial^2\varphi(s,t)}{\partial s^2}=-\left(\frac{L^2}{I}\right)\int_{-\infty}^{t}J(t-\tau)\left\{\frac{\partial[R(\tau)\sin\varphi(s,\tau)]}{\partial\tau}\right\}\mathrm{d}\tau \tag{36}$$

We note that the boundary conditions for this problem are

$$\varphi(0,t)=0 \tag{37a}$$

$$M(1,t)=aR(t)\cos\varphi(1,t) \tag{37b}$$

where, for a rigid "extension,"

$$\alpha(t)=\varphi(1,t) \tag{37c}$$

Through the use of Eqs. (10) and (12a), the second boundary condition [Eq. (37b)] can, after nondimensionalization, be expressed entirely in terms of φ by

$$\frac{\partial\varphi(1,t)}{\partial s}=\left(\frac{L}{I}\right)\int_{-\infty}^{t}J(t-\tau)\left\{\frac{\partial[aR(\tau)\cos\varphi(1,\tau)]}{\partial\tau}\right\}\mathrm{d}\tau \tag{37d}$$

Assuming that the column is undeformed for $\tau<0$ and that following the procedure detailed in Eqs. (15-25) again yield a solution of the form of Eq. (25) except that, in this case,

$$\theta(s,t)=\left(\frac{sa}{L}\right)\cos\varphi(1,t)+\int_0^1 g(s,u)\sin\varphi(u,t)\mathrm{d}u \tag{38}$$

Note that the nonlinear boundary term $\cos\varphi(1,t)$ appears inside the convolution integral as well as in the integrated term of Eq. (25).

Under a constant load P it is again plausible to assume that $\varphi(s,\tau)$ will be a nondecreasing function with respect to τ. Thus, in addition to Eqs. (26) and (27), we note

$$\sin\varphi(s,0^+)\le\sin\varphi(s,\tau)\le\sin\varphi(s,t) \tag{39}$$

Because of the differences in bounding behavior in Eqs. (27) and (39), the convolution integral of the general solution [Eq. (25)] is split into two separate integrals that are bounded individually.

Substitution of the appropriate bounding functions from Eqs. (27) and (39) into Eq. (38) and substitution of these results into Eq. (25) yield, after integration and rearrangement of terms

$$\begin{aligned}\varphi_{lb}(s,t)=J(0)\left(\frac{PL^2}{I}\right)\Bigg\{&\int_0^1 g(s,u)\sin\varphi(u,t)\mathrm{d}u\\&+\left[\frac{J(t)}{J(0)}\right]\left(\frac{sa}{L}\right)\cos\varphi(1,t)\\&+\left[\frac{J(t)}{J(0)}-1\right]\int_0^1 g(s,u)\sin\varphi(u,0^+)\mathrm{d}u\Bigg\}\end{aligned} \tag{40a}$$

$$\begin{aligned}\varphi_{ub}(s,t)=J(0)\left(\frac{PL^2}{I}\right)\Bigg\{&\left(\frac{sa}{L}\right)\cos\varphi(1,t)\\&+\left[\frac{J(t)}{J(0)}-1\right]\left(\frac{sa}{L}\right)\cos\varphi(1,0^+)\\&+\left[\frac{J(t)}{J(0)}\right]\int_0^1 g(s,u)\sin\varphi(u,t)\mathrm{d}u\Bigg\}\end{aligned} \tag{40b}$$

Numerical evaluation of Eqs. (40), as well as the exact solution given by Eqs. (25) and (38), is accomplished in the same manner as the prior example. Figures 6 and 7 present the results of these computations for the ideal "limited creep" model used in Refs. 5 and 6 and illustrated on Fig. 5. For this particular constitutive model, the creep compliance $J(t)$ has the form

$$\frac{J(t)}{J(0)}=1+\left(\frac{E_2}{E_1}\right)e^{-\mu t} \tag{41a}$$

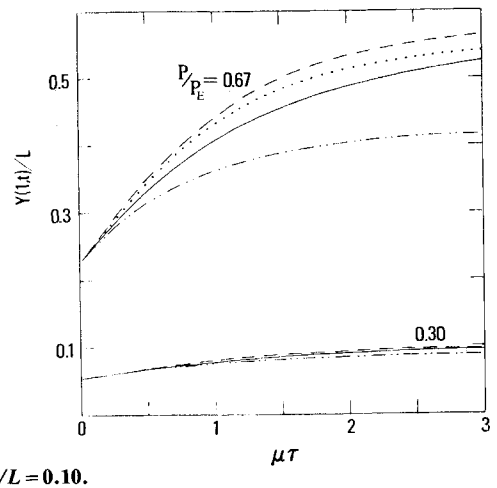

a) $a/L = 0.10$.

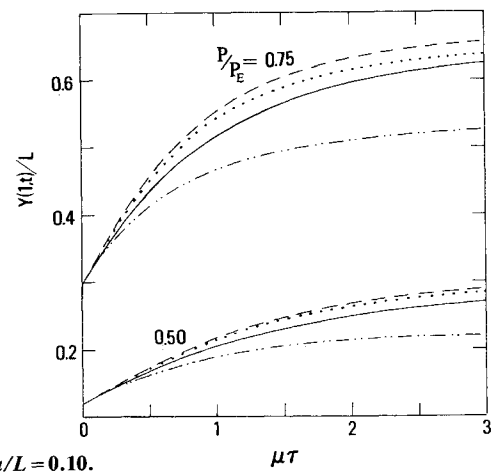

b) $a/L = 0.10$.

Fig. 7 End deflection of the eceentrically loaded cantilever column for the three-element model.

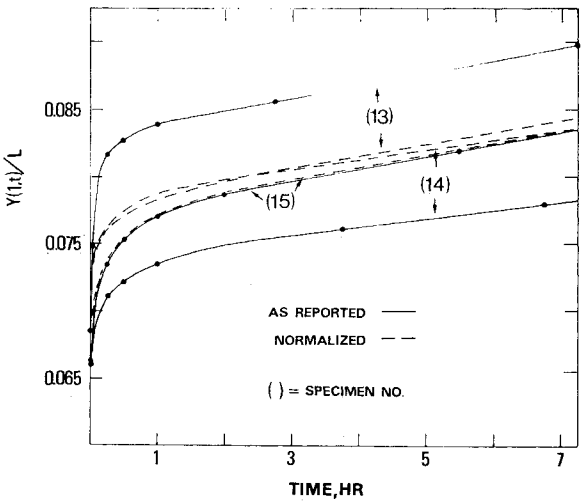

a) $P/P_E = 0.40$ and $a/L = 0.07$.

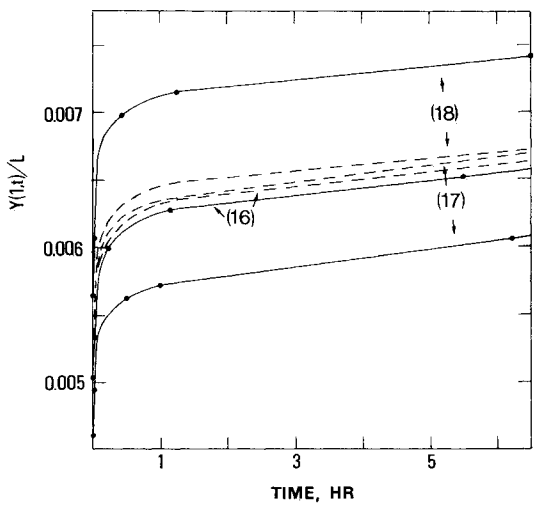

b) $P/P_E = 0.125$ and $a/L = 0.03$.

Fig. 8 Reported and normalized experimental data for the six-element model.

where we have employed

$$J(0) = 1/E_2 \tag{41b}$$

$$\mu = E_1/\eta_1 \tag{41c}$$

Figure 6 presents results for $E_2/E_1 = 0.5$ and $a/L = 0.01$ for a range of load ratios. In this figure, and all succeeding ones, we employ a viscoelastic "Euler" load P_E to nondimensionalize the loading, where

$$P_E = \frac{\pi^2 I}{4J(0)L^2} \tag{42}$$

For comparison, this figure also includes results from a "standard" quasielastic solution φ_{qe} of the general form

$$\varphi_{qe}(s,t) = \left(\frac{PL^2}{I}\right) J(t)\theta(s,t) \tag{43}$$

where the various functions on the right-hand side are as previously defined.

It can be observed that the quasielastic solution is almost identical to the upper-bound result for the load ratios of 0.67 and 0.75. At the load ratio of 0.50, the upper-bound and quasielastic results differ only in the fourth decimal place. Thus, only the upper-bound result has been indicated in the figure for this load case.

Although the upper-bound and quasielastic results compare favorably with each other, neither of them nor the lower-bound solution provides a good approximation to the exact result except at the lowest load ratio, 0.50. Thus, reliance on only a quasielastic type of solution, especially for the higher loading instances, could lead to erroneous results.

With only a quasielastic solution, it is impossible to determine its accuracy without calculating the exact solution. Thus, it is not possible to assess the magnitude or character (i.e., conservative or nonconservative) of the potential errors. In contrast, the amount of separation between the bounding solutions provides such a capability. The narrow separation evident at a load ratio of 0.50 might well provide sufficiently accurate results without resorting to the more involved analysis. The significant differences between the bounds at the higher loads, instead, indicate that exact solutions must be determined for accurate results.

Figure 7 provides results for the same ratio of modulii, but for a load eccentricity of 0.10. Again, at the lowest load ratio (0.30), the quasielastic and upper-bound solutions are virtually indistinguishable and only the upper bound is indicated.

Comparison of Figs. 6 and 7 illustrates that the increase in load eccentricity generates several pronounced effects. The quasielastic solution, in general, tends to provide a more accurate prediction of behavior at all load levels for the higher load eccentricity. Additionally, the larger eccentricity tends to decrease the spread between the upper- and lower-bound approximations. This is not, however, a completely general

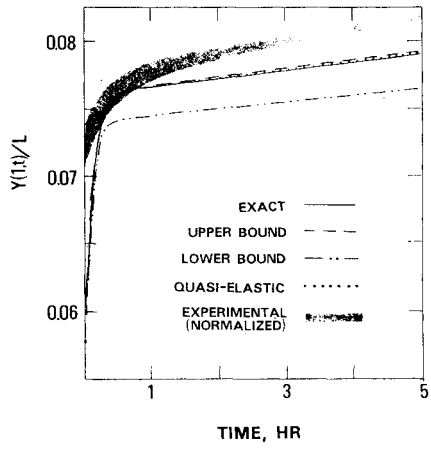

a) $P/P_E = 0.40$ and $a/L = 0.07$.

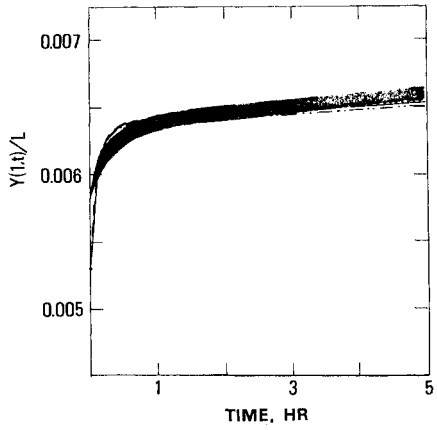

b) $P/P_E = 0.125$ and $a/L = 0.03$.

Fig. 9 End deflection of the eccentrically loaded cantilever column for the six-element model.

trend, since at the load ratio of 0.50 the bounding is much more narrow for the lower eccentricity case.

Since some experimental results also are available,[5,6] a comparison with these data is worthwhile. Figure 8 provides reported as well as "normalized" data for two load-eccentricity cases. The normalized curves are generated by adding the relative displacement of a specimen from its time $= 0^+$ (i.e., 10 or 20 s deflection) to the average 0^+ displacement of that test group. In this way, the significant differences between the observed results in a test group due solely to the differences in "instantaneous" deflection could be eliminated. As indicated in the figure, this virtually eliminates the substantial differences between observed results.

Based on data from four point bending tests the specimen material (PTFE G-700) was modeled[6] as a six-element "unlimited creep" type of material. The numerical form for the creep compliance is given by

$$J(t)/J(0) = 1 + 3.7 \times 10^{-4} t + 0.17(1 - e^{-9.02t}) + 0.13(1 - e^{-0.04t}) \quad (44)$$

Figure 9 presents the comparison of the exact quasielastic, upper- and lower-bound results to the normalized test data of Fig. 8. Note that, while there is an apparent significant difference between observed and calculated results for the higher-load case, differences in the 0^+ deflection account for most of it. The average reported "instantaneous" nondimensional deflection was 0.0633, whereas the calculated value was only 0.0580. If the various results were to be normalized to eliminate this difference, the test data band would completely overlap the calculated results. However, using such a procedure for the lower-load case would decrease the correlation indicated on Fig. 8. Since the observed "instantaneous" deflection was only 0.00504, normalizing the data to the calculated deflection of 0.00530 would move the band of test data so that it would be somewhat above the calculated results. The main conclusion to be drawn is that, qualitatively, the calculated results agree with the observed data. Exact comparability is, however, hindered by the large differences in initial displacement evident in the test data.

Conclusions

A methodology is presented wherein problems of isothermal linear viscoelastic behavior, formulated using nonlinear kinematic measures of deformation, may be analyzed through the use of a bounding procedure. The bounding solutions developed by this technique are similar in form to that of a time-dependent elasticity problem. As such, numerical solutions may be generated without requiring the computation of convolution integrals of the entire history of deformation. In one of the examples considered, it is shown that this results in an increase in computational efficiency more than 30 times greater by comparison to the more traditional approach.

It is also demonstrated that the bounding procedure provides reasonably accurate results for a variety of loading conditions. In those cases where narrow bounds cannot be established, it is shown that a standard type quasielastic approach is not necessarily more reliable. The clear implication of the wide bounds is that the more involved traditional approach must be employed if highly accurate results are required.

As presented, the bounding technique can be directly employed for problems where the governing functions may be characterized as either nonincreasing or nondecreasing functions with respect to time. However, the range of applicability potentially can be expanded to include some forms of multimodal functions. In general, this would require that these functions be capable of being characterized, at least in a piecewise manner, as a sequence of unimodal segments. Similar to the procedure that was employed in the second example, each of these segments would then be bounded individually. The degree of accuracy that might be obtained using such a procedure, however, requires further study.

Acknowledgments

This work was performed under NASA Grant NAG 3-534. The financial support provided by NASA is gratefully acknowledged by the authors. Special thanks are extended to Dr. C. C. Chamis of the NASA Lewis Research Center for his encouragement and for the many meaningful and fruitful discussions.

References

[1]Schapery, R. A., "Approximate Methods of Transform Inversion for Viscoelastic Stress Analysis," *Proceedings of 4th U. S. Congress on Applied Mechanics*, Vol. 2, 1962, pp. 1075-1085.

[2]Rogers, T. G. and Lee, E. H., "On the Finite Deflection of a Viscoelastic Cantilever," *Proceedings of 4th U. S. Congress on Applied Mechanics*, Vol. 2, 1962, pp. 977-987.

[3]Schapery, R. A., "A Method of Viscoelastic Stress Analysis Using Elastic Solutions," *Journal of the Franklin Institute*, Vol. 279, No. 4, 1985, pp. 268-289.

[4]Vinogradov, A. M., "Nonlinear Effects in Creep Buckling Analysis of Columns," *Journal of Engineering Mechanics, ASCE*, Vol. 111, No. 6, 1985, pp. 757-767.

[5]Vinogradov, A. M. and Wijeweera, H., "Theoretical and Experimental Studies on Creep Buckling," *Proceedings of AIAA/ASME/ASCE/AHS 26th Structures, Structural Dynamics and Materials Conference*, Vol. 1, 1985, pp. 160-164.

[6]Wijeweera, H., "Creep Buckling of Initially Imperfect Linear Viscoelastic Columns," M.S. Thesis, Dept. of Civil Engineering, University of Calgary, Canada, 1984.